Extrusion-based Additive Manufacturing of Zirconium Carbide for Nuclear Fuel Cell Structures

Guang Yang[a], Yuhui Xiang[b], Thomas Poirier[c], Narges Malmir[a], Tiankai Yao[d], Nikhil Churi[e], Brian Taylor[f], James H. Edgar[c], Dong Lin[b,*], Shuting Lei[a,*]

[a] *Department of Industrial and Manufacturing Systems Engineering, Kansas State University, Manhattan, KS 66506, USA*
[b] *School of Mechanical, Industrial, and Manufacturing Engineering, Oregon State University, Corvallis, OR 97331, USA*
[c] *Tim Taylor Department of Chemical Engineering, Kansas State University, Manhattan, KS 66506, USA*
[d] *Idaho National Laboratory, Idaho Falls, ID 83415, USA*
[e] *Woodbury School of Business, Utah Valley University, Orem, UT 84058, USA*
[f] *NASA Marshall Space Flight Center, Advanced Propulsion Systems, Huntsville, AL 35808, USA*
[*] *Corresponding authors*
E-mail address: dong.lin@oregonstate.edu (D. Lin), lei@ksu.edu (S. Lei).

ABSTRACT

Nuclear thermal propulsion relies on heating hydrogen propellant using nuclear fuel to generate thrust for spacecraft propulsion. Ceramic fuel elements like zirconium carbide (ZrC) offer advantages over metals due to their high melting points and high temperature stability. The primary function of ZrC in this context is to provide structural integrity and stability to the nuclear fuel, especially under high-temperature and high-radiation conditions. Vanadium carbide (VC), a nonradioactive surrogate with similar properties, has also emerged for research purposes. Recent advancements include utilizing VC as a sintering additive for ZrC, enhancing densification and mechanical properties. Traditional ZrC fabrication methods struggle with intricate geometries, but additive manufacturing (AM), specifically extrusion-based methods, revolutionizes ceramic fabrication by offering material flexibility, multi-material printing, minimal waste, and rapid prototyping. This study explores extrusion-based AM for the fabrication of ZrC nuclear fuel cell structures. Experimental findings highlight the impact of Nano Crystalline Cellulose (NCC) and VC additives on 3D-printed ZrC ceramics: higher NCC concentrations improves ink recovery and reduces deformation during the printing process but excessive NCC leading to increased porosity after sintering process; VC additives mitigate decreased mechanical properties caused by higher NCC content, emphasizing the crucial role of ink composition and additive selection in achieving desired material properties for broader applications. These insights pave the way for innovative approaches in AM structures for nuclear propulsion and other high-performance applications. The integration of AM technologies with advanced materials like ZrC and tailored additives represents a significant step towards efficient and sustainable propulsion systems for future space exploration missions.

Keywords: Zirconium carbide, Additive Manufacturing, Three-interval thixotropy test

1. Introduction

Nuclear thermal propulsion works by using nuclear fuel to heat a hydrogen propellant to generate thrust and propel a spacecraft. The higher the gas temperature the larger the specific impulse, hence the better rocket performance. In this regard, ceramic fuel elements have advantage over their metallic counterparts because of their high melting points, high chemical stability, superior corrosion resistance, and high fission product retention [1]. Among ceramic materials for nuclear fuel applications, zirconium carbide (ZrC) is a versatile material with a remarkable combination of properties, including its high melting point, exceptional thermal stability, and efficient neutron absorption capabilities, making it a desirable candidate for such a purpose [2]. In nuclear fuel pellets, ZrC is commonly used as a matrix material for fuel rods. This matrix serves as a protective barrier around the nuclear fuel, which can be in the form of uranium or other fissile materials [3]. However, working with radioactive materials such as uranium carbide requires strict regulations and safety measures, which makes it impractical to handle in a regular research lab. Therefore, vanadium carbide (VC) is chosen as a surrogate material for uranium carbide because it is nonradioactive, and has a similar crystal structure as uranium carbide [4].

Recent advancements in materials science and engineering have introduced the use of vanadium carbide as a sintering additive for zirconium carbide. This development represents a significant improvement in increasing grain size and densification [5]. Vanadium carbides possess remarkable properties, including high melting points and excellent thermal and mechanical stability, making them an ideal candidate for enhancing the sintering process of ZrC, a material known for its exceptional hardness and refractory nature [6]. The incorporation of vanadium carbides as a sintering aid has led to enhanced densification and improved mechanical properties of the resulting composite materials.

In the realm of ZrC ceramics, the conventional fabrication methods have long grappled with the challenge of producing intricate geometries [7-9]. Crafting complex shapes often necessitated costly machining of these dense, erosion-resistant, and brittle composites, utilizing ultra-hard (diamond) tooling [10]. However, the landscape of ceramics fabrication has undergone a profound transformation with the emergence of additive manufacturing (AM), or 3D printing, technology. Various AM techniques, such as binder jetting [11, 12], laser powder bed fusion (LBPF) [13, 14], Stereolithography (SLA) [15-18] and material extrusion [19, 20], have become integral to the field.

Among these methods, extrusion-based AM stands out for its distinctive advantages. Unlike traditional approaches, it offers unmatched material flexibility, accommodating a broad spectrum of materials ranging from polymers and ceramics to metals and bioinks. This versatility empowers the creation of intricate, tailor-made structures designed for specific applications. Furthermore, it facilitates multi-material printing, enabling the construction of composite structures endowed with diverse properties. Noteworthy is its minimal waste production, swift prototyping capabilities, and seamless customization, making it highly coveted in research, development, and various industries. These unique merits position extrusion-based AM as a frontrunner in the field, sparking innovation and in both manufacturing and scientific endeavors.

In this study, we use an extrusion-based AM method for manufacturing zirconium carbide nuclear fuel cell structures. The experimental results highlighted significant findings regarding the impact of NCC and VC additives on the properties of 3D-printed ZrC ceramics. The rheological analysis demonstrated that higher NCC concentrations in the ink formulation resulted in the improved ink recovery times, leading to enhanced self-supporting capacity during printing and reduced deformation of printed structures. Microstructural analysis revealed a delicate balance, where lower NCC concentrations promoted denser microstructures with reduced porosity, thus enhancing mechanical properties such as compressive strength and hardness. However, excessive NCC content increased porosity, adversely affecting structural integrity. Mechanical testing further confirmed these trends, showing that while higher NCC content generally decreased elastic modulus and compressive strength, the inclusion of VC additives helped mitigate these effects within specific concentration ranges, showcasing improved mechanical properties. These results emphasized the critical role of ink composition and additive selection in achieving desired material properties for advanced applications in 3D-printed ceramics.

2. Experimental section

2.1 Ink Preparation

As illustrated in Fig. 1a, ink was prepared by mixing zirconium carbide powders (with a d50 value of 3-5 micrometers, Standford Advanced Materials, Lake Forest, CA) and vanadium carbide powders (average particle size ≤ 2 micrometers, Sigma-Aldrich, Saint Louis, MO) in DI water at a total solid concentration of 70 wt. %. Darvan C-N (Vanderbilt Minerals, Norwalk, CT) as the dispersant was added at 1 wt. % based on the total weight of the slurry. The incorporation of NCC as a binder and thickener enables precise control over the ink's viscosity, ensuring its printability. The mixture was homogenized for 24 hours using magnetic stirring at 350 rpm. Subsequently, NanoCrystalline Cellulose (CelluForce, Canada) was added as a binder and rheology modifier to adjust the ink's viscosity. The ink was stirred magnetically at 350 rpm and mechanically at 800 RPM until it stabilized.

2.2 Design of Experiments (DOE)

To systematically study the impact of both NCC and VC as additives for ZrC, a comprehensive 2-variable 3-level full factorial experimental design was employed. This experimental approach, outlined in Table 1, involved varying each variable at low, medium, and high levels, resulting in a total of 9 different inks. These inks were meticulously prepared and printed using consistent parameters as detailed in previous section, providing a structured foundation for analyzing the intricate relationship between material properties and the additives of the ink.

Table 1. Design of experiments with two major additives for the ink

Ink #	Concentration of NCC	Concentration of VC
1	Low (100mg/mL)	Low (0 vol%)
2	Low (100mg/mL)	Medium (10 vol%)
3	Low (100mg/mL)	High (20 vol%)
4	Medium (150mg/mL)	Low (0 vol%)
5	Medium (150mg/mL)	Medium (10 vol%)
6	Medium (150mg/mL)	High (20 vol%)
7	High (200mg/mL)	Low (0 vol%)
8	High (200mg/mL)	Medium (10 vol%)
9	High (200mg/mL)	High (20 vol%)

2.3 Rheology Properties Testing

The suspension rheology was characterized using an MCR92 modular compact rheometer (Anton Paar, Vemon Hills, IL) with a 25 mm parallel plate geometry and a gap of 500 μm. The three-interval thixotropy test was performed at the shear rate at 0.1 reciprocal seconds (0.1/s) and 5 reciprocal seconds (5/s) at a constant temperature of 25 °C.

2.4 3D Printing and Post-processing

Prior to printing, the ink was prepared by loading it into a 30 mL syringe and agitating it using a vortex mixer to remove air bubbles. Following this, the slicing software Cura was utilized to design internal structures and establish printing parameters. The prepared syringe was then connected to a customized 3D printer for the AM process, adhering to the predefined patterns illustrated in Fig. 1b & c. The ink was dispensed through a 0.413 mm nozzle at a printing speed of 15 mm/s, with a layer height set at 0.5 mm for the printed object. Subsequently, the printed sample was allowed to air-dry naturally at room temperature (25°C) for a duration of 12 hours.

To enhance the strength of the printed samples, a meticulous sintering process was employed involving controlled heating, pressure, and a specialized environment. As depicted in Fig. 1d, the furnace chamber underwent three purge cycles: initially reaching a pressure of less than $5x10^{-2}$ torr to eliminate air, then reducing the argon backfill to less than $5x10^{-5}$ torr, and finally decreasing another backfill to less than $5x10^{-3}$ torr before filling the furnace to approximately 862 torr with 99% Argon. Following these purges, an argon flow of 500 sccm was initiated before commencing temperature control. The furnace was gradually heated to 1450°C at 10°C per minute monitored using a type C thermocouple, then further raised to 1750°C at 5°C per

minute under pyrometer control. After dwelling at 1750°C for 2 hours, the samples were cooled to room temperature over 6 hours, completing the sintering process.

2.5 Scanning Electron Microscopy (SEM) Characterization

To assess the microstructural features of the 3D printed ZrC samples, an SEM analysis was conducted using the FEI QUANTA 3D DualBeam SEM/Focused Ion Beam (FIB) system (FEI, Hillsboro, OR). Sample preparation involved mounting the ZrC specimens on SEM stubs with conductive double-sided adhesive tape to ensure stability and high-resolution imaging, followed by sputter-coating with a 10 nm thick gold layer to enhance conductivity and prevent charging effects. The SEM was operated at an accelerating voltage of 30 kV, balancing image resolution and beam penetration. High-resolution SEM images of the ZrC surfaces and cross-sections were captured at various magnifications, providing a detailed view of the specimens' microstructure.

The porosity of the samples was characterized using ImageJ software. Initially, the Threshold function was applied to convert the image to binary, effectively isolating the porosity from the background. Subsequently, Particle Analysis was conducted to quantify the empty area, with the resulting percentage of empty area representing the porosity of the samples.

2.6 Mechanical Properties Testing

The uniaxial compressive test was conducted using the Compact Table-Top Universal Tester (Shimadzu, Kyoto, Japan). Cylindrical samples, 10 mm in diameter and 10 mm in height, were prepared and polished with ISO P120 sandpapers. The test was performed in displacement control mode at a rate of 1 mm/min until ultimate failure.

The hardness test was carried out on the same machine, replacing modules with a Vickers indenter. It operated in displacement control mode at 1 mm/min until reaching 4 kgf, followed by a 15-second hold time. Indentation results were analyzed using an optical microscope.

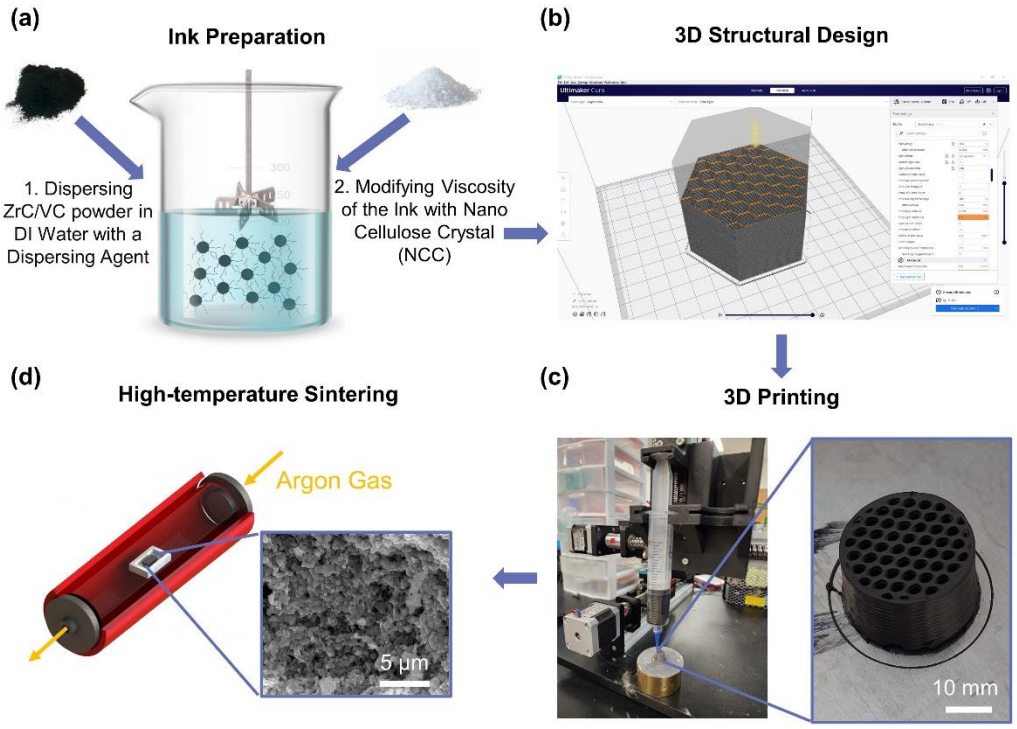

Fig. 1. Schematic of the 3D printing process. a) Ink preparation. b) 3D structural design. c) 3D printing. d) High-temperature sintering.

3. Results and discussion

3.1. Rheological Characteristics of the Ink

To achieve self-supporting 3D structures with precise shape fidelity, it is imperative to consider the transition kinetics from a fluid-like flow to a solid-like behavior. Rapid recovery plays a crucial role in ensuring that the printed paste maintains its shape, restoring its elastic behavior and preventing excessive flow immediately after extrusion. This recovery can be quantified by assessing viscosity as shear stress quickly decreases from values exceeding the flow point to low, near-rest shear values.

The three-interval thixotropy test (3ITT) is a rheological assessment that provides this critical information and can be conducted in either rotational or oscillatory modes. It simulates an extrusion-based printing process by employing five consecutive steps with varying shear rates (as depicted in Fig. 2a): 1. A low shear rate within the linear viscoelastic range of the amplitude sweep, mimicking the ink's resting state as it slowly advances through the 3D printing cartridge. 2. An immediate increase in shear rate, resembling the ink's behavior during rapid acceleration. 3. A high shear rate exceeding the flow point, positioned as close as possible to the maximum shear rate, emulating the extrusion process through a small nozzle. 4. A prompt decrease in shear rate to an extremely low level, enabling the ink to rapidly recover to its high-viscosity state. 5. A return to a low shear rate to replicate the ink's resting state after deposition.

The objective of these tests is to evaluate the rapid recovery of solid-like behavior to maintain nozzle shape and ensure both accurate printing fidelity and the self-supporting capacity of the

printed structure. As depicted in Fig 2b, the 3ITT was performed on inks with varying amounts of NCC added. In the initial interval, the rheometer shear rate was set at 0.1 (1/s) for 20 seconds, simulating the ink's slow advancement through the syringe. The viscosity briefly increased due to the acceleration of the rheometer's rotating disks before stabilizing. In the subsequent interval, the disk shear rate abruptly surged to 5 (1/s) for 20 seconds, imitating ink extrusion from the nozzle. During this phase, the ink exhibited fluid-like behavior with a rapid viscosity decrease. In the third interval, the disk shear rate returned to 0.1 (1/s), and the ink's viscosity rapidly recovered to its initial level.

Generally, with increasing NCC content, the ink's viscosity exhibited synchronized growth at both high and low shear rates. However, the critical finding in these tests, as illustrated in Fig. 2c, was the significant reduction in ink recovery time with higher NCC concentrations. Within the first 5 seconds, inks with 150 and 200 mg/mL NCC added recovered to over 90% of its original viscosity, whereas the ink with 100 mg/mL NCC added only reached 83.62% of its original viscosity. After 15 seconds of recovery, the former ink regained 99% of its initial viscosity, while the latter recovered only 93.7%. This rapid ink recovery time is pivotal for printing outcomes as it significantly influences the self-supporting capacity of the printed structure. Fig. 2d further corroborates this characteristic of the ink. Clearly, the ink with low NCC content struggled to maintain the structure, leading to substantial deformation in the bottom structure. In contrast, inks with higher NCC concentrations exhibited robust self-supporting behavior, ensuring stable and accurate printing results.

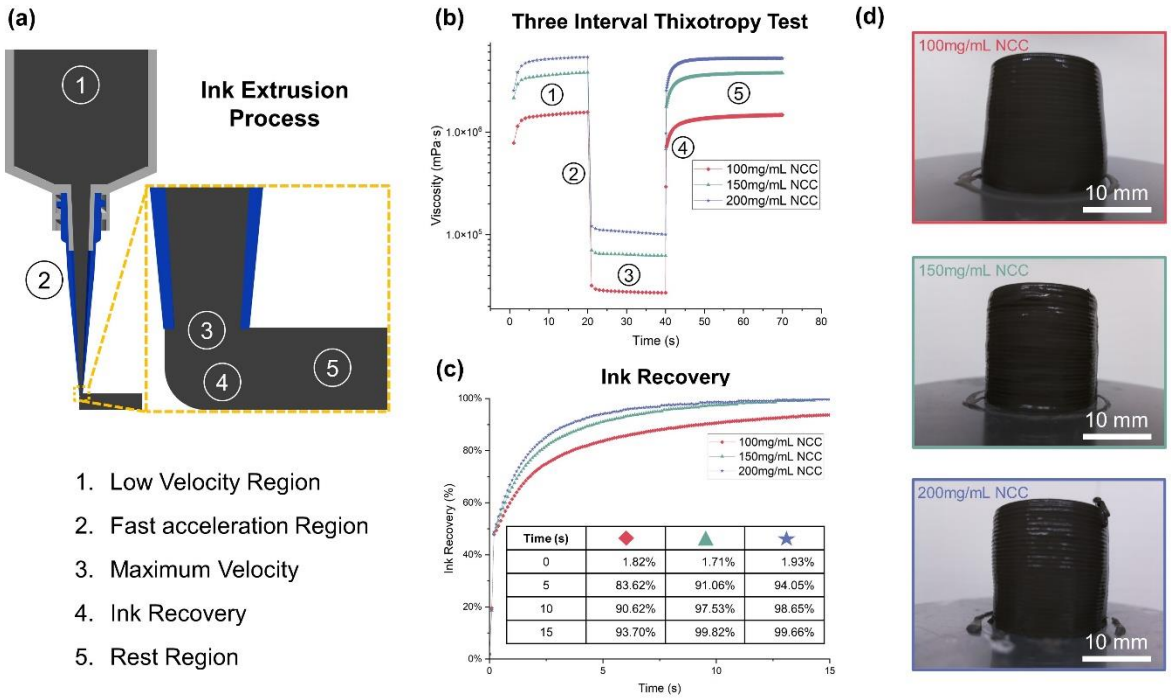

Fig. 2. a) Ink extrusion process. b) 3ITT result. c) Ink recovery time results. d) Printed ZrC cylindrical sample with different NCC added.

After the samples were printed, they were air-dried at room temperature (25°C) for 12 hours. Time-lapse images were captured every minute during the drying process, as depicted in Fig. 3. The top surface diameter, bottom surface diameter, and height of the samples were continuously monitored, enabling the calculation of volumetric shrinkage, as illustrated in Fig. 3b. Analyzing three different conditions with varying NCC concentrations revealed a clear trend: the shrinkage decreased from 26.54% to 22.03% as NCC content increased from 100 mg/mL to 200 mg/mL. Notably, the total drying time was also reduced by approximately 2 hours.

The deformation of the printed samples was assessed both before and after the drying process. Because of variations in the ink's self-supporting capability, adding more layers during deposition concentrated greater weight on the bottom layers, resulting in shape deformations, particularly noticeable at the sample's base layers. To quantify this deformation, a deviation angle was introduced, measured between the outer surface of the printed cylindrical sample and the vertical reference line. As demonstrated in Fig. 3c, the sample with 100 mg/mL NCC exhibited the largest deviation angle of 6.6°, which increased to 7.35° after drying. However, as the NCC concentration increased, the deviation angle decreased significantly by 56.6% to 89.5%. Remarkably, in the case of the sample with 200 mg/mL NCC, the deviation angle reduced from 1.21° to 0.77° after drying. This reduction highlights the substantial improvement in ink's self-supporting capacity due to the increased NCC content, resulting in superior printing and drying outcomes.

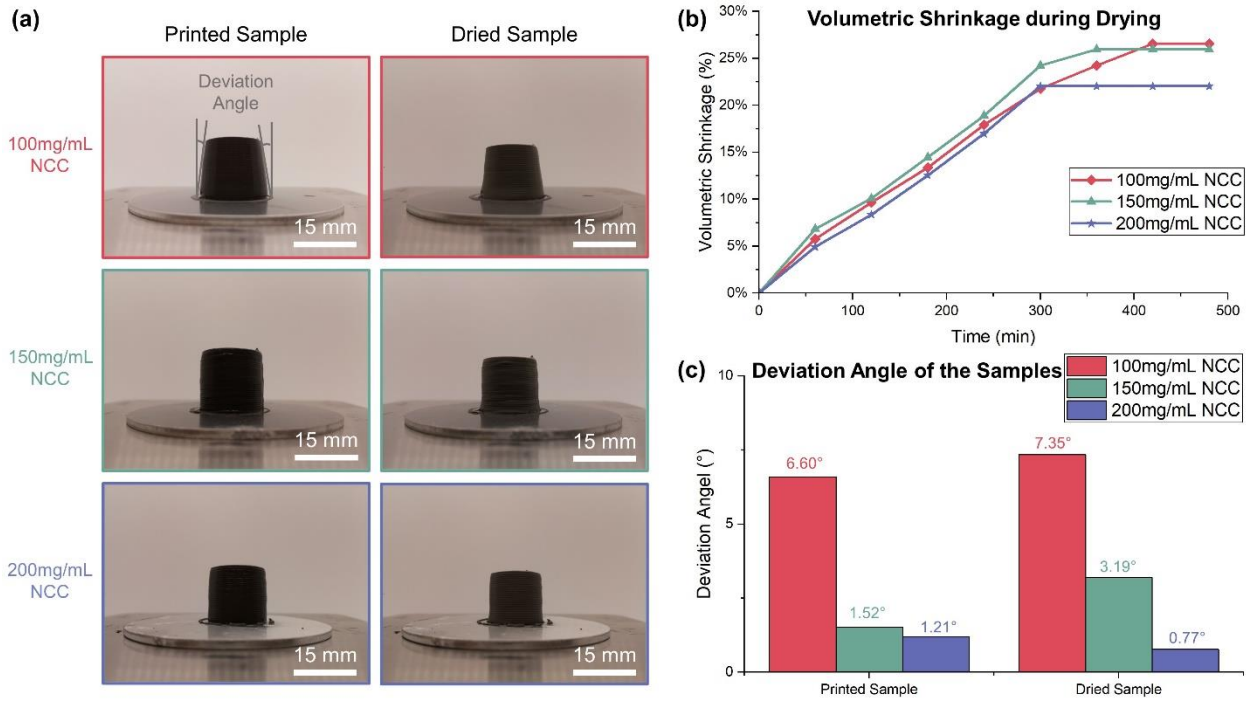

Fig. 3. a) Images of samples before and after drying process. b) Volumetric shrinkage results during the drying process. c) Deviation angle of the samples before and after drying process.

3.2. Microstructure Analysis

The microstructure of 3D-printed ZrC (Zirconium Carbide) samples is a critical aspect that directly influences the material's mechanical properties and overall performance. This microstructure encompasses various factors such as grain size, particle distribution, and porosity, all of which play important roles on determining how the material behaves under different conditions. After sintering the samples at 1750°C, a high-magnification SEM examination of their cross-sections revealed significant insights into their microstructural characteristics. Figure 4a provides a visual representation of how the microstructure varies under different conditions, particularly with the addition of NCC. When a low concentration of NCC (100mg/mL) is added, it fosters a closer bond among ceramic particles, resulting in larger grain sizes and reduced porosity. This closer bonding is the key for enhancing the material's mechanical properties and structural integrity. On the contrary, higher concentrations of NCC lead to increased porosity due to the presence of more voids or gaps among the ceramic particles. These gaps hinder the fusion of particles during sintering, resulting in smaller grain sizes and compromised material properties. The reason behind this behavior lies in the decomposition of NCC during the sintering process. As NCC decomposes, it creates additional space within the particles, making it more challenging for them to sinter effectively. This phenomenon is reflected in the observed microstructural changes and corresponding mechanical properties shown in the next section.

To accurately quantify the porosity, sophisticated image analysis techniques were employed using ImageJ software. Figure 4b illustrates the process, where SEM images were meticulously processed to isolate areas of interest containing microstructures. By applying the Threshold function to convert these images into binary form, the porosity areas were effectively separated from the background. Subsequent Particle Analysis provided quantitative data on the empty areas, representing the porosity levels in the samples. To ensure the reliability of the data, multiple images (three per condition) were analyzed, validating the observed trends. Samples with 100mg/mL NCC exhibited the lowest porosity levels (approximately 4%-6%), indicating a denser and more compact microstructure. As the NCC concentration increased to 200mg/mL, porosity levels escalated to 12% and higher, signifying a more porous microstructure with compromised material properties.

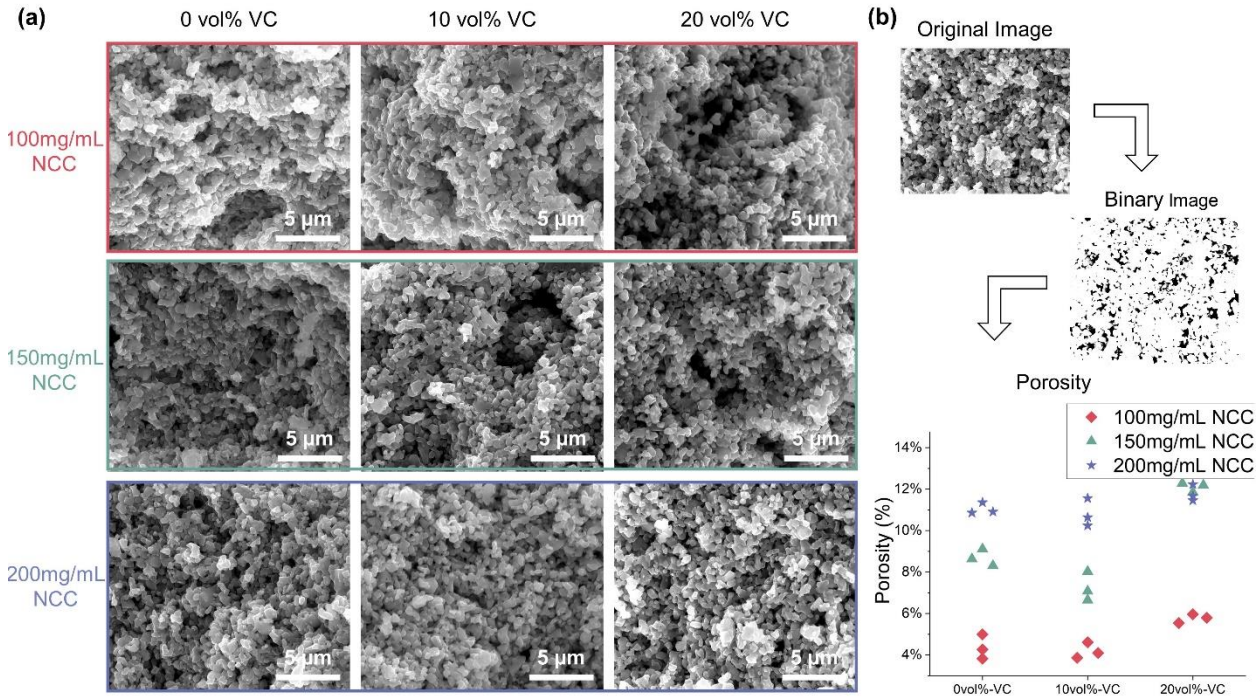

Fig. 4. a) SEM images depicting cross-sectional views under various conditions. b) Description of the porosity calculation method.

3.3. Mechanical Properties

In the realm of 3D printing for advanced applications, such as nuclear fuel cells, understanding and optimizing the mechanical properties of materials is paramount. Zirconium carbide (ZrC), a promising candidate for these purposes, demands meticulous attention to its mechanical traits. Key factors such as elastic modulus, representing a material's ability to deform under stress and return to its original shape, are critical for ensuring structural integrity and stability within the intricate designs of nuclear fuel cells. Compressive strength, which measures the capacity of a material or structure to withstand loads tending to reduce size, is vital in enduring extreme conditions within nuclear reactors. Additionally, hardness, indicating resistance to deformation and wear, is essential for durability and long-term performance. Achieving a delicate balance among these properties is imperative for the successful 3D printing of ZrC components, ensuring they endure the harsh nuclear environment while maintaining efficiency and safety in fuel cell applications.

Fig. 5 shows the mechanical properties tests for the sintered ZrC samples. The typical stress-strain curve of sintered cylindrical ZrC samples under uniaxial compressive test is shown in Fig. 5a. Unlike ductile materials, which deform plastically under stress, the ZrC samples exhibited no plastic deformation before fracturing. Due to the brittle nature of the ceramics, the samples failed instantly after getting to their maximum strength and random cracks could be observed through

the entire sample. The elastic modulus and compressive strength were obtained from the stress-strain curve generated during the compressive test.

The elastic modulus, a key parameter indicating a material's stiffness, was calculated from the linear elastic segment of the stress-strain curve, as illustrated in Fig. 5b. Variations in the elastic modulus were observed under different conditions. Specifically, increasing the NCC concentration from 100mg/mL to 150mg/mL caused a significant decrease in the elastic modulus. Surprisingly, further increasing the NCC concentration to 200mg/mL did not result in as substantial a reduction in the elastic modulus. Additionally, incorporating a 10 vol% concentration of VC led to the highest elastic modulus observed for each condition, with an average increase ranging from 8.7% to 15.8%. However, increasing the VC concentration to 20 vol. % led to a subsequent decrease in the elastic modulus, sometimes even surpassing samples without added VC.

The compressive strength, as shown in Fig. 5c, indicating the maximum stress a material can withstand without failure, was determined from the point on the stress-strain curve where the stress significantly deviated from linearity and began to decrease. Despite inherent fluctuations due to the brittle nature of ZrC samples, the trend closely followed that of the elastic modulus. Generally, an increase in NCC content led to a decrease in compressive strength. However, the introduction of a 10 vol. % concentration of VC resulted in notably higher compressive strength compared to other tested conditions, with an average increase ranging from 24.7% to 48.9%.

Finally, micro indentation tests were conducted on samples under nine distinct conditions employing Vickers' indentation method with a diamond indenter. The results of the hardness tests are depicted in Fig. 5d, indicating consistent outcomes. Increased NCC content corresponded to reduced hardness, whereas a 10 vol. % concentration of VC exhibited comparatively superior hardness compared to other conditions. The addition of 10 vol. % of VC resulted in an average hardness increase ranging from 37.2% to 52.5%.

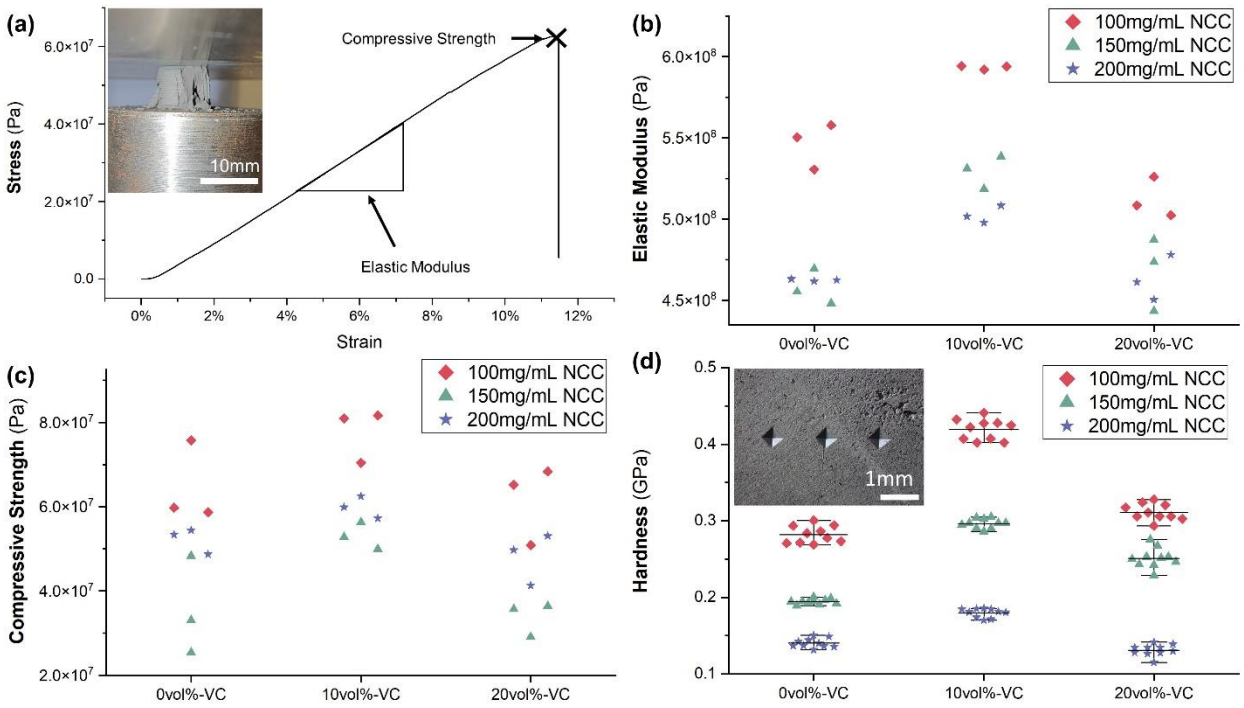

Fig. 5. Mechanical properties of the sintered samples a) Uniaxial compressive test. b) Elastic modulus. c) Compressive strength. c) Micro indentation tests.

4. Conclusions and future work

The comprehensive study on the preparation and characterization of ZrC/VC ink for 3D printing has provided valuable insights into optimizing ink formulations and understanding the resulting material properties. Through systematic ink preparation and rheological analysis, it was observed that the addition of NCC as a binder and thickener significantly influenced ink viscosity and recovery behavior during the printing processes. Higher concentrations of NCC led to improved ink recovery times, enhancing the self-supporting capacity of printed structures and reducing deformation.

The microstructure analysis of 3D-printed ZrC samples revealed a delicate balance between NCC concentration and the resulting porosity levels. Lower concentrations of NCC facilitated denser microstructures with reduced porosity, positively impacting mechanical properties such as compressive strength and hardness. However, excessive NCC content resulted in increased porosity, affecting material integrity and mechanical performance.

Mechanical testing, including uniaxial compressive tests and hardness evaluations, highlighted the influence of NCC and VC concentrations on material properties. While higher NCC content generally reduced elastic modulus and compressive strength, the incorporation of vanadium carbide (VC) additives mitigated these effects, showcasing improved mechanical properties under specific concentration ranges.

Overall, this study underscores the importance of precise ink formulation, rheological control, and additive selection for achieving desired material properties in 3D-printed ZrC ceramics. Future research directions may focus on further optimizing ink compositions, exploring

additional additives, and investigating post-printing treatments to enhance the performance and applicability of printed ZrC ceramic components in advanced engineering applications.

Declaration of Competing Interest

The authors declared that there is no conflict of interest.

Acknowledgments

This material is based upon work supported by NSF No. 2309995, and National Aeronautics and Space Administration under Cooperative Agreement No. 80NSSC22M0261 and 80NSSC22M0221.

References

[1] J. Marra, Advanced ceramic materials for next-generation nuclear applications, IOP Conference Series: Materials Science and Engineering, IOP Publishing, 2011, pp. 162001.
[2] Y. Katoh, G. Vasudevamurthy, T. Nozawa, L.L. Snead, Properties of zirconium carbide for nuclear fuel applications, Journal of Nuclear Materials, 441 (2013) 718-742.
[3] S. Hamilton, N.D. Jerred, R. Scott, M. Bachhav, T. Yao, V.M. Miller, Diffusion study of uranium mononitride/zirconium carbide composite for space nuclear propulsion, Journal of Nuclear Materials, 583 (2023) 154535.
[4] B. Taylor, B. Emrich, D. Tucker, M. Barnes, N. Donders, K. Benensky, Study of a Tricarbide Grooved Ring Fuel Element for Nuclear Thermal Propulsion, 2018.
[5] X.-G. Wang, J.-X. Liu, Y.-M. Kan, G.-J. Zhang, Effect of solid solution formation on densification of hot-pressed ZrC ceramics with MC (M= V, Nb, and Ta) additions, Journal of the European Ceramic Society, 32 (2012) 1795-1802.
[6] L. Wu, T. Yao, Y. Wang, J. Zhang, F. Xiao, B. Liao, Understanding the mechanical properties of vanadium carbides: Nano-indentation measurement and first-principles calculations, Journal of alloys and compounds, 548 (2013) 60-64.
[7] D. Gosset, M. Dollé, D. Simeone, G. Baldinozzi, L. Thomé, Structural evolution of zirconium carbide under ion irradiation, Journal of nuclear materials, 373 (2008) 123-129.
[8] G.-M. Song, Y.-J. Wang, Y. Zhou, The mechanical and thermophysical properties of ZrC/W composites at elevated temperature, Materials Science and Engineering: A, 334 (2002) 223-232.
[9] T. Zhang, Y. Wang, Y. Zhou, T. Lei, G. Song, Elevated temperature compressive failure behavior of a 30 vol.% ZrCp/W composite, International Journal of Refractory Metals and Hard Materials, 25 (2007) 445-450.
[10] C.B. Carter, M.G. Norton, Ceramic materials: science and engineering, Springer2007.
[11] J. Gonzalez, J. Mireles, Y. Lin, R.B. Wicker, Characterization of ceramic components fabricated using binder jetting additive manufacturing technology, Ceramics International, 42 (2016) 10559-10564.
[12] W. Du, X. Ren, C. Ma, Z. Pei, Ceramic binder jetting additive manufacturing: Particle coating for increasing powder sinterability and part strength, Materials Letters, 234 (2019) 327-330.
[13] K. Shahzad, J. Deckers, J.-P. Kruth, J. Vleugels, Additive manufacturing of alumina parts by indirect selective laser sintering and post processing, Journal of Materials Processing Technology, 213 (2013) 1484-1494.
[14] S.L. Sing, W.Y. Yeong, F.E. Wiria, B.Y. Tay, Z. Zhao, L. Zhao, Z. Tian, S. Yang, Direct selective laser sintering and melting of ceramics: a review, Rapid Prototyping Journal, 23 (2017) 611-623.
[15] B. Mansfield, S. Torres, T. Yu, D. Wu, A review on additive manufacturing of ceramics, International Manufacturing Science and Engineering Conference, American Society of Mechanical Engineers, 2019, pp. V001T001A001.

[16] Z. Chen, Z. Li, J. Li, C. Liu, C. Lao, Y. Fu, C. Liu, Y. Li, P. Wang, Y. He, 3D printing of ceramics: A review, Journal of the European Ceramic Society, 39 (2019) 661-687.
[17] H. Wu, Y. Cheng, W. Liu, R. He, M. Zhou, S. Wu, X. Song, Y. Chen, Effect of the particle size and the debinding process on the density of alumina ceramics fabricated by 3D printing based on stereolithography, Ceramics International, 42 (2016) 17290-17294.
[18] H. Xing, B. Zou, S. Li, X. Fu, Study on surface quality, precision and mechanical properties of 3D printed ZrO2 ceramic components by laser scanning stereolithography, Ceramics International, 43 (2017) 16340-16347.
[19] H. Shao, D. Zhao, T. Lin, J. He, J. Wu, 3D gel-printing of zirconia ceramic parts, Ceramics International, 43 (2017) 13938-13942.
[20] M. Faes, J. Vleugels, F. Vogeler, E. Ferraris, Extrusion-based additive manufacturing of ZrO2 using photoinitiated polymerization, CIRP Journal of Manufacturing Science and Technology, 14 (2016) 28-34.